Waste and Biomass Valorization
https://doi.org/10.1007/s12649-026-03513-2

ORIGINAL PAPER

Sustainable Valorisation of Red and White Grape Pomace Via Sequential Supercritical Fluid Extraction for Selective Recovery of High-value Bioactives

Carla Da Porto[1] · **Andrea Natolino**[1]

Received: 29 August 2025 / Accepted: 2 February 2026

Abstract

This study investigates a sequential supercritical fluid extraction process for the selective recovery of bioactive compounds from white (WGP) and red grape pomace (RGP). Supercritical CO_2 (280 bar, 70 °C, 10 kg h^{-1} CO_2) was first applied to extract nonpolar compounds, mainly policosanol, achieving concentrations of 3398 mg $kgDM^{-1}$ in WGP and 1841 mg $kgDM^{-1}$ in RGP. This step was followed by extraction with CO_2 and a co-solvent (80 bar, 40 °C, 6 kg h^{-1} CO_2, 10% w/w ethanol–water mixture, 57% v/v) to recover polar phenolics, yielding 1879 mg GAE 100 gDM^{-1} in WGP and 2160 mg GAE 100 gDM^{-1} in RGP. Extraction kinetics were successfully described using the Broken and Intact Cell model, indicating internal diffusion as the main rate-limiting mechanism, which was significantly reduced by co-solvent addition. Overall, the sequential SFE process represents an efficient and sustainable strategy for grape pomace valorization.

Graphical Abstract

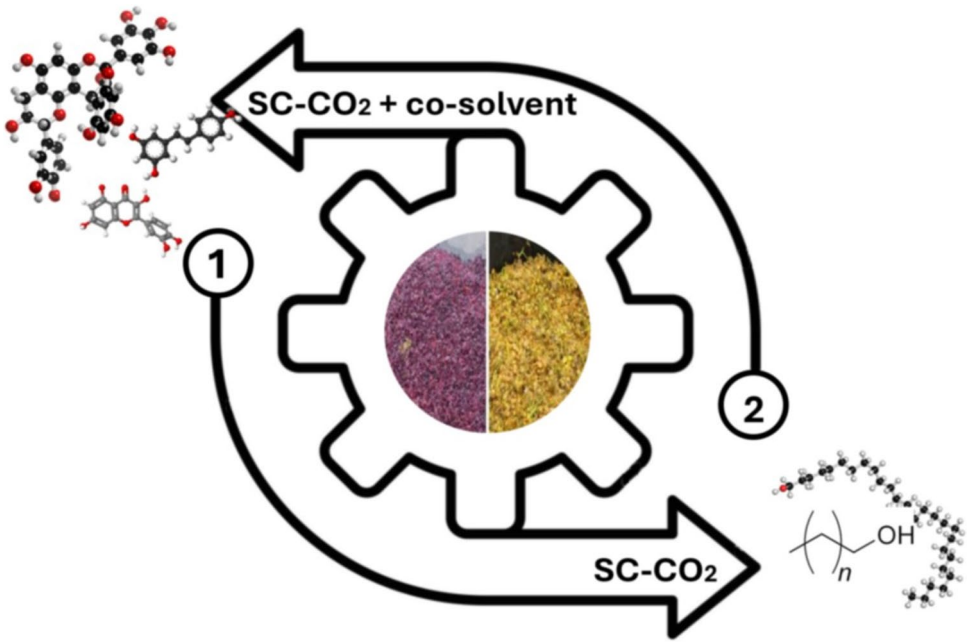

Keywords Broken and intact cell model · Grape pomace · Supercritical CO_2 extraction · Kinetic modeling · Polyphenols · Policosanol

Extended author information available on the last page of the article

Published online: 17 February 2026

Nomenclature

a_0	Specific surface area per unit volume of extraction bed (m^{-1})
a_s	Specific area between intact and broken cells (m^{-1})
c_u	Solute content in the untreated solid (kg(solute) kg(solid) $^{-1}$)
d_p	Particle diameter (m)
e	Extraction yield (kg(extract) kg(insoluble solid)$^{-1}$)
k_f	Fluid-phase mass transfer coefficient (s^{-1})
k_s	Solid-phase mass transfer coefficient (s^{-1})
N	Solid load in the extractor (kg)
N_m	Load of insoluble solid (kg)
q	Relative amount of the passed solvent (kg(solvent) kg(insoluble solid)$^{-1}$)
q_m	Relative amount of passed solvent at the end of CER period (kg(solvent) kg(insoluble solid)$^{-1}$)
q_n	Relative amount of passed solvent at the end of FER period(kg(solvent) kg(insoluble solid)$^{-1}$)
$\dot{Q}$	Solvent flow rate (kg/s)
r	Grinding efficiency (fraction of broken cells)
t	Extraction time (min)
t_{CER}	Extraction time at the end of CER period (min)
t_{FER}	Extraction time at the end of FER period (min)
x_i	Concentration in broken cells (kg(solute) kg (insoluble solid)$^{-1}$)
x_u	Concentration in the untreated solid (kg(solute) kg (insoluble solid)$^{-1}$)
y	Fluid phase concentration (kg(solute) kg (solvent)$^{-1}$)
y_0	Initial fluid-phase concentration (kg(solute) kg (solvent)$^{-1}$)
y_s	Solubility (kg(solute) kg (solvent)$^{-1}$)

Greek letters

γ	Solvent to matrix ratio in the bed (kg(solvent) kg(insoluble solid)$^{-1}$)
ρ_a	Solid apparent density (kg/m^3)
ρ_f	Solvent density (kg/m^3)
ρ_s	Solid real density (kg/m^3)
θ_e	Dimensionless external mass transfer resistance
θ_i	Dimensionless internal mass transfer resistance
$\mathcal{E}$	Bed void fraction

Statement of Novelty

The development of a sequential supercritical fluid extraction (SFE) process that enables the selective recovery of nonpolar policosanol followed by polar phenolic compounds within a single integrated framework represents a novel approach for the valorization of grape pomace. Furthermore, the modeling and evaluation of kinetic parameters for such a sequential SFE process—explicitly accounting for the dynamic evolution of mass-transfer mechanisms across successive extraction stages—has not been previously reported.

Introduction

Grape pomace is the main solid by-product of the wine industry, with an estimated annual global production of 6–7 million tons (fresh weight) in recent years [1]. Generated during the pressing stage of winemaking, it consists primarily of grape skins, seeds, and stems. Its composition varies according to grape variety, vinification practices, and pressing intensity [2]. Among the constituents of grape pomace, polyphenols have received considerable attention due to their strong antioxidant activity and broad applications in the food, pharmaceutical, and cosmetic industries [3–8].

In contrast, policosanol—a group of long-chain aliphatic alcohols (C20–C36) in the wax layer of grape skins and seeds [9–11] —had not previously been studied in grape pomace. To the best of our knowledge, our recent work was the first to identify and investigate grape pomace as a source of policosanol, thereby opening new perspectives for its valorization [12]. Policosanol, originally isolated from sugarcane wax and beeswax [13], are now widely used in dietary supplements, food additives, cosmetics, pharmaceuticals, and animal feed [14–18].

The valorization of grape pomace as a cost-effective source of bioactive compounds is often constrained by the efficiency and selectivity of the extraction method. Supercritical fluid extraction (SFE), particularly with supercritical carbon dioxide (SC–CO_2), has emerged as a promising technology due to its mild operating conditions, non-toxicity, chemical inertness, and ability to produce solvent-free, high-purity extracts. Although SC–CO_2 is naturally well suited for nonpolar compounds, its solvating power can be enhanced for polar and moderately polar molecules by adding small amounts of co-solvents [19–27].

The present work aims to model and evaluate the kinetic parameters of a sequential SFE process for the selective recovery of bioactive compounds from red and white grape pomace.

Materials and Methods

Grape Pomace Characterization

White grape pomace (WGP) and red grape pomace (RGP) were collected in the Friuli Venezia-Giulia region (Italy). They were dried in an air circulation oven at 40 °C for 24 h and stored in dark conditions at 4 °C until they were used. Moisture content was determined by oven drying to constant weight at 105 °C. Prior to SC–CO_2 extraction,

the grape pomaces were milled by a domestic grinder and particles characterized by size classification in a standard sifter with several mesh sizes. Mean particle diameter was determined according to Sauter's equation [28] to a set of fractions within previous mesh sized. The true density (ρ_s) of raw material was determined by helium gas pycnometry (Pycnomatic ATC, Thermo Electron Corporation, Milan, Italy). The apparent density (ρ_a) was calculated by dividing the feed mass by the vessel volume. The porosity of the bed (ε) was calculated as $(1-\rho_a/\rho_s)$. WGP and RGP were characterized for their physicochemical properties before and after SC–CO_2 extraction as shown in Table 1.

SFE Pilot-Scale Sequential Process

The pilot-plant used was an SCF100 Series 3 PLC-GR-DLMP model (Separeco S.r.L., Pinerolo, Italy) located at University of Udine. It is equipped with a 1 L cylindrical extraction vessel, followed by two separators (each with a capacity of 0.3 L), and a CO_2 storage tank that enabled CO_2 recycling throughout the process (Fig. 1).

SC–CO_2 Extraction of Nonpolar Fraction

SC–CO_2 extraction of WGP and RGP was carried out at 280 bar, 70 °C and 10 kg/h CO_2 flow rate [12]. An amount of 0.1 kg of ground pomace (WGP or RGP) was introduced into the extractor between two thick layers of glass beads (mean

Table 1 Physicochemical properties of white and red grape pomace before and after SC–CO_2 extraction

	White grape pomace		Red grape pomace	
	Raw material	After SC–CO_2 extraction	Raw material	After SC–CO_2 extraction
Moisture (% w/w)	10.96 ± 0.17	7.66 ± 0.32	7.43 ± 0.39	4.30 ± 0.10
Mean particle diameter (mm)	0.663 ± 0.014	0.570 ± 0.008	0.613 ± 0.009	0.536 ± 0.007
True density (kg/m^3)	1262 ± 19	1055 ± 174	1271 ± 19	960 ± 147
Apparent density (kg/m^3)	293.95 ± 0.17	98.42 ± 0.36	293.82 ± 0.34	98.26 ± 0.19
Porosity (ε)	0.767 ± 0.004	0.905 ± 0.015	0.769 ± 0.003	0.896 ± 0.015

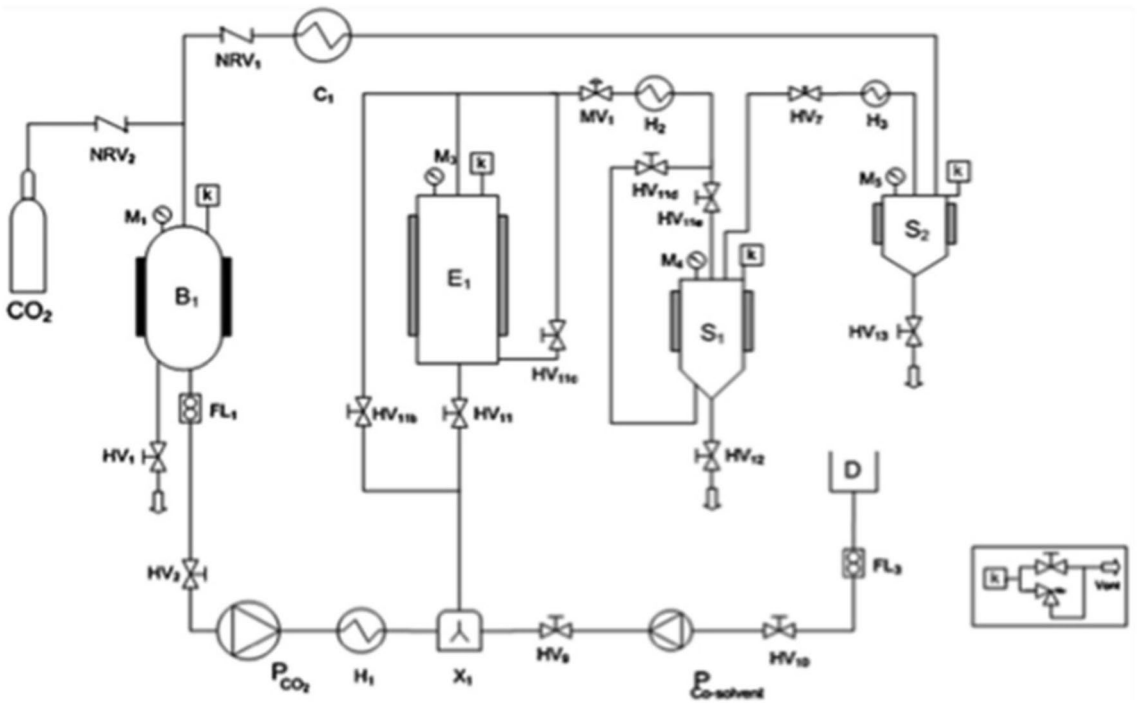

Fig. 1 SFE pilot plant flow sheet. (B_1) Storage tank; (E_1) extraction vessel; (S_1,S_2) separators; (H#) heater exchangers; (C_1) condenser; (HV#) Hand valves; (MV_1) membrane valve; (NVR#) no return valves; (*P*) diaphragm pumps; (F_1) flowmeter; (M#) manometers; (k) safety devices; (FL_1) Coriolis mass flowmeter; (D) cosolvent storage tank; (X#) mixer

diameter of 0.005 m) placed at the bottom and top of the extractor. Sampling of extracts was conducted at the outlet of S_1. The extraction time was fixed at 180 min. At intervals of 30 min, samples of SC–CO_2 grape pomace extracts were collected in volumetric flasks and their weights were measured using a precise analytical balance (± 0.0001 g). This allowed for the determination of extraction yields, then used for the overall extraction curves (OECs). The extraction yield was expressed as yield (% w/w) = [(weight of the extract)/(weight of the dried sample) × 100].

SC–CO_2 Plus Co-solvent Extraction of Polar Fraction

After SC–CO_2 extraction of nonpolar fraction, SC–CO_2 plus co-solvent extraction was carried out at 80 bar, 40 °C, 6 kg/h CO_2 flow rate and 10% w/w of ethanol – water mixture at 57% (v/v) as co-solvent [5]. The extraction time was fixed at 480 min. Aliquots of grape pomace extract were collected during extractions in a volumetric flask at intervals of 30 min, to assess several data points for the overall extraction curves (OECs). After removal of the co-solvent with a rotary evaporator (Buchi, B465, Switzerland) at 45 °C, the extracts were weighed for yield determination.

Modeling for Sequential SFE Process

The cumulative mass of extract, e, as a function of time (or solvent mass ratio, q), can be described by the Broken and Intact Cells (BIC) model [29–33]. The extraction process is divided into three characteristic periods:

(i) Constant Extraction Rate (CER) period

$$e = qy_s\left[1 - exp\left(-\frac{1}{\theta_e}\right)\right] \text{for } 0 \le \text{q} < \text{qm} \tag{1}$$

(ii) Falling Extraction Rate (FER) period

$$e = qy_s - rx_i\theta_e \exp\left(\frac{\beta}{\theta_e} ln\left\{1 + \frac{1}{r}\left[exp\left(\frac{q - q_m}{\theta_i\gamma}\right) - 1\right]\right\} - \frac{1}{\theta_e}\right) \quad \text{for qm} \le \text{q} < \text{qn} \tag{2}$$

(iii) Diffusion-Controlled (DC) period

$$e = x_u\left[1 - \beta ln\left\{1 + (1 - r)\left[exp\left(\frac{1}{\beta}\right) - 1\right] exp\left(\frac{q - q_m}{\gamma\theta_i}\right)\right\}\right] \quad \text{for q} \ge \text{qn} \tag{3}$$

The model requires the following relationships:

$$\theta_i = \frac{(1 - \varepsilon)\dot{Q}}{\gamma k_s a_s N_m} \tag{4}$$

$$\theta_e = \frac{\varepsilon\dot{Q}}{\gamma k_f a_0 N_m} \tag{5}$$

$$q_m = \frac{rx_u\theta_e}{y_s} \tag{6}$$

$$q_n = q_m + \gamma\theta_i ln\left[1 - r + rexp\left(\frac{1}{\beta}\right)\right] \tag{7}$$

$$\beta = \frac{\gamma\theta_i y_s}{x_u} \tag{8}$$

The adjustable parameters θ_e, θ_i, r, k_s and k_f were calculated by minimizing the sum of least squares between the experimental and calculated values of e.

Preliminary experimental parameters are determined as follows:

$$e_{exp} = \frac{E}{N_m} \tag{9}$$

$$q = \frac{M}{N_m} \tag{10}$$

where E is the amount of extract (kg), M is the mass of solvent passed (kg), and N_m is the mass of insoluble solid:

$$N_m = \left(1 - c_u\right)N \tag{11}$$

Here, c_u is the solute fraction in the untreated solid (equal to the asymptotic extraction yield at infinite time), obtained by preliminary fitting.The solute weight fraction in the solid (x_u) is then:

$$x_u = \frac{c_u}{1 - c_u} \tag{12}$$

The bed characteristics, porosity (Ɛ), specific surface area per unit volume of extraction bed (a_0) and solvent to matrix ratio (γ) are:

$$\varepsilon = 1 - \frac{\rho_a}{\rho_s} \tag{13}$$

$$a_0 = 6\frac{1 - \varepsilon}{d} \tag{14}$$

$$\gamma = \frac{\rho_f\varepsilon}{\rho_s(1 - \varepsilon)} \tag{15}$$

Chemical Analyses

Chemicals

Carbon dioxide (mass fraction purity 0.999 in the liquid phase was supplied by Sapio S.r.l. (Udine, Italy). Sep-Pak Plus tC18 cartridge WAT 036810 and WAT036800 were purchased from Waters (Milan, Italy). The standards used for GC–MS analysis, 1-hexacosanol (C26), 1-octacosanol (C28) and 1- triacontanol (C30) were purchased from Sigma-Aldrich (Milan, Italy). Bis (trimethylsilyl) trifluoro acetamide (BSTFA) from Carlo Erba (Milan, Italy) was used as the derivatization reagent. All other solvents and reagents used in analytical determinations were Sigma-Aldrich Co. (Milan, Italy), proanalysis type.

Total Phenolic Content

To eliminate interference from sugars, non-volatile acids, and amino acids during total phenol quantification, the grape pomace extracts were purified using C18 solid-phase extraction cartridges. Total phenolic content (TPC) was then determined using the Folin–Ciocalteu method, as described by Yu et al. [34]. All analyses were conducted in triplicate, and results were expressed as milligrams of gallic acid equivalents per 100 g of dry matter (mg GAE/100 g DM).

GC–MS Analysis of Policosanol

Sample preparation was carried out according to the method described by Haim et al. [35], with minor modifications. Briefly, 100 µL of each SC–CO_2 extract was mixed with 100 µL of a betulin solution (100 µg/mL in heptane), used as an internal standard, and 1 mL of ethanolic sodium hydroxide (1 N NaOH in 80:20 ethanol/water, v/v). The mixture was vortexed for 30 s and subjected to saponification at 80 °C for 1 h. Polycosanols were extracted via liquid–liquid extraction by adding 2 mL of heptane, vortexing for 1 min, and heating at 70 °C for 10 min. The organic phase was collected into a 10 mL test tube. This extraction step was repeated three times, and the combined organic layers were evaporated to dryness under a nitrogen stream. The resulting residue was reconstituted in 500 µL of BSTFA (N,O-bis(trimethylsilyl)trifluoroacetamide) and derivatized at 80 °C for 20 min. A 1 µL aliquot of the derivatized sample was then injected into the GC–MS system for analysis.

GC–MS analysis was performed on a Shimadzu GC-2010 gas chromatograph coupled to a GCMS-QP2010 mass spectrometer (Shimadzu, Kyoto, Japan). Separation was achieved on an HP-5 MS capillary column (30 m × 250 µm I.D., 0.25 µm film thickness; Agilent Technologies, CA, USA). The oven temperature program was as follows: initial temperature of 200 °C, increased at 10 °C/min to 300 °C, and held for 10 min. Helium was used as the carrier gas at a flow rate of 1 mL/min. Injections were made in splitless mode at 300 °C; the transfer line and ion source were maintained at 300 °C and 230 °C, respectively. Mass spectrometry was carried out in selected ion monitoring (SIM) mode with electron ionization at 70 eV. A solvent delay of 6 min was applied, and the mass range scanned was m/z 40–600.

Compound identification was based on comparison of retention times and target ions with NIST MS 107 and NIST 21 spectral libraries and literature references (https://webbook.nist.gov/chemistry/). The monitored ions were m/z 439 for 1-hexacosanol, 467 for 1-octacosanol, and 495 for 1-triacontanol. Quantification of 1-hexacosanol (C26), 1-octacosanol (C28), and 1-triacontanol (C30) was achieved using external calibration curves generated over a concentration range of 15–300 µg/mL. All measurements were performed in triplicate.

Results and Discussion

Modeling and Evaluation of Kinetic Parameters in Sequential SFE

The experimental and modeled SFE overall extraction curves (OECs) of the nonpolar and polar fraction from WGP and RGP are presented in Fig. 2a, b, respectively. These curves are crucial for optimizing supercritical fluid extraction processes since allow to understand the kinetics and influence of parameters such as temperature, pressure, and solvent flow rate on extraction efficiency. The average absolute relative deviation (AARD) values ranging from 0.214 to 3.511% indicate the strong predictive capability of the BIC model in describing the extraction kinetics of the fractions from both types of grape pomace (Table 2).

Figure 2a shows that both OECs of the nonpolar fraction from WGP and RGP exhibit an initial constant-extraction rate (CER) period lasting 25 min, followed by a falling extraction rate (FER) period. Up to 25 min, the OECs for both grape pomaces overlap, indicating similar mass transfer behavior during the CER phase, which is driven by convection in the fluid phase. Beyond this point, the curves begin to diverge and the extraction rate decline as the easily accessible solute is depleted. During the FER period the mass transfer mechanism shifts from convection-dominated to diffusion-dominated. This period is influenced by the differing structural and compositional properties of WGP and RGP matrices, affecting internal and external mass transfer. By comparing the OECs, it is evident that the maximum extraction yields—7.25 ± 0.24% w/w for WGP and 8.19 ± 0.12% w/w for RGP—are achieved after 180 min. However, approximately 90% of the final global yield is

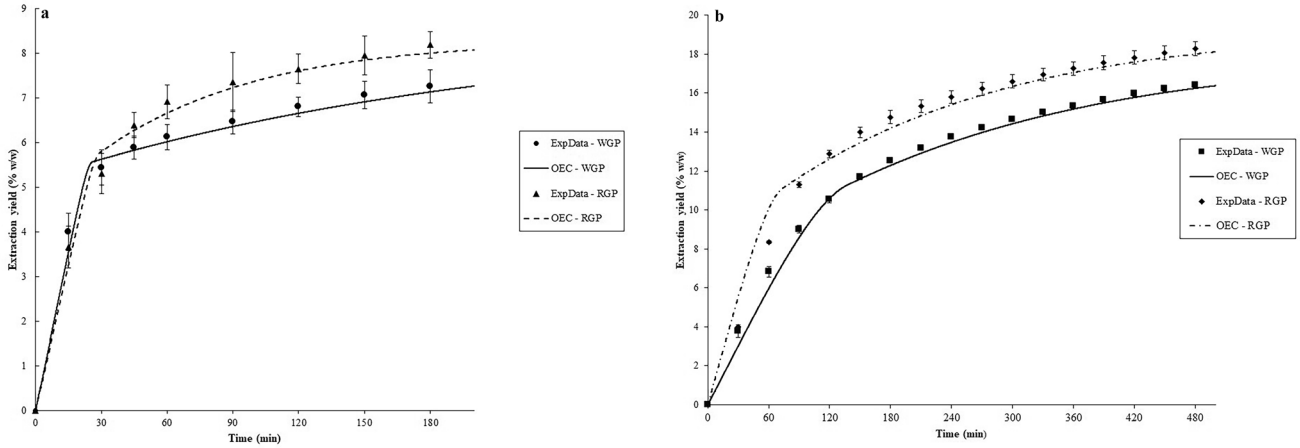

Fig. 2 Experimental (symbols) and modeled (lines) overall extraction curves (OECs) of SC–CO2 extraction (280 bar/ 70° C/10.0 kg/h CO_2 flow rate) (a), and SC–CO_2 extraction + co-solvent (80 bar/ 40 °C /6.0 kg/h CO_2 flow rate/ 10% (w/w) ethanol – water mixture at 57% (v/v)) (b) from white (WGP) and red (RGP) grape pomace

already obtained within the first 90 min of extraction for both raw materials.

The OECs of the polar fraction from WGP and RGP in Fig. 2b show that the CER period for WGP is shorter than that observed for RGP, indicating a more prolonged phase of efficient mass transfer in RGP. This may be due to RGP higher total phenolic content, which could result in more extractable compounds being readily available during the initial stages of extraction, governed by external mass transfer. The distinct structural and compositional characteristics of WGP and RGP, which influence both internal and external mass transfer mechanisms, contributed to differences observed during the FER period. Comparison of the OECs reveals that the maximum extraction yields were $16.42 \pm 0.10\%$ w/w for WGP and $18.28 \pm 0.14\%$ w/w for RGP, both achieved after 480 min.

Table 2 reports the kinetic parameters of the sequential SFE process estimated by fitting the experimental data to the OECs obtained from SC–CO_2 extraction (first step) and SC–CO_2 + co-solvent extraction (second step) for WGP and RGP.

As reported in Table 2 for SC–CO_2 extraction, both WGP and RGP exhibited similar values of the overall mass transfer coefficient (k_f), suggesting that the external mass transfer resistance (film diffusion) between the solid particle surface and the flowing CO_2 is comparable for both grape pomaces. However, the solubility of the nonpolar fraction in supercritical CO_2 (y_s) is slightly higher in WGP ($4.816 \cdot 10^{-3}$ kg/kgCO_2) than in RGP ($4.404 \cdot 10^{-3}$ kg/kgCO_2). This suggests that WGP contains a greater amount of extractable compounds, or that they dissolve more readily in supercritical CO_2 than those in RGP.

The application of Sovová's model [29–31] yielded two mass transfer coefficients: $k_f a_0$, describing solute transfer in the fluid phase, and $k_s a_s$, representing solute transfer within the solid phase. The initial mass transfer coefficients ($k_f a_0$) for WGP and RGP were $3.7706 \cdot 10^{-2}$ and $3.7606 \cdot 10^{-2}$ $\cdot s^{-1}$, respectively. The nearly identical values indicate that the initial mass transfer rates are comparable for both matrices, as reflected by the similar slopes of the extraction curves (Fig. 2a). This interpretation is further supported by the dimensionless external mass transfer parameter, Θ_e, calculated as 0.1033 for WGP and 0.1032 for RGP.

The solid-phase mass transfer coefficient ($k_s a_s$) was higher in RGP ($5.8917 \cdot 10^{-5}$ s^{-1}) than in WGP ($1.9330 \cdot 10^{-5}$ s^{-1}). This difference can be attributed to the intrinsic structural and compositional properties of the pomaces, likely influenced by the winemaking process [36, 37], which affect the ability of supercritical CO_2 to penetrate and diffuse through the internal porous structure of the solid matrix. Furthermore, the fact that $k_s a_s$ is about three orders of magnitude lower than $k_f a_0$ for both pomaces highlights the predominance of internal diffusion resistance in the overall process. This is further supported by the high values of the internal mass transfer resistance parameter Θ_i, calculated as 613.910 for WGP and 200.069 for RGP.

The similar q_m values of WGP (14.351 kg CO_2 per kg pomace) and RGP (15.225 kg CO_2 per kg pomace) indicate that both pomaces required a similar solvent-to-feed ratio to reach the end of the CER period, where easily accessible solutes on the particle surface are removed. This suggests comparable surface accessibility and external mass transfer efficiency during the initial phase for both pomaces, as previously reported.

In contrast, the slightly higher q_n value for RGP (177.391 kg CO_2 per kg pomace) compared to WGP (157.827 kg CO_2 per kg pomace) indicates that extraction from intact cells in RGP requires more solvent, reflecting

Table 2 Kinetic parameters of the sequential SFE process from white and red grape pomace

Grape Pomace	Sequential SFE	Kinetic parameters									
		k_f (-)	Y_s (kg/kg_{co2})	r (-)	K_fa_0 (s^{-1})	k_sa_s (s^{-1})	θ_e (-)	θ_i (-)	q_m (kg_{co2}/kg)	q_n (kg_{co2}/kg)	AARD (%)
White	$SC–CO_2$ extraction	$1.7839\ 10^{-5}$	$4.816\ 10^{-3}$	0.6314	$3.7706\ 10^{-2}$	$1.9330\ 10^{-5}$	0.1033	613.910	14.351	157.827	0.214
Red		$1.7789\ 10^{-5}$	$4.404\ 10^{-3}$	0.6343	$3.7606\ 10^{-2}$	$5.8917\ 10^{-5}$	0.1032	200.069	15.225	177.391	0.812
White	$SC–CO_2$ etraction + co-solvent	$2.6038\ 10^{-5}$	$1.0357\ 10^{-3}$	0.5442	$2.1103\ 10^{-2}$	$5.6413\ 10^{-6}$	0.3563	111.268	44.842	190.801	1.060
Red		$2.8563\ 10^{-5}$	$1.9202\ 10^{-3}$	0.5189	$2.2321\ 10^{-2}$	$6.3305\ 10^{-6}$	0.3308	101.00	23.471	102.441	3.511

stronger internal mass transfer resistance likely associated with its more complex internal structure, which slows the release of solutes from within the particles.

As reported in Table 2 for $SC–CO_2$ + co-solvent extraction, the overall mass transfer coefficient (k_f) results to be $2.6038 \cdot 10^{-5}$ for WGP and $2.8563 \cdot 10^{-5}$ for RGP. However, the k_f values of $SC–CO_2$ + co-solvent extraction resulted higher than the k_f values of $SC–CO_2$ extraction both for WGP and RGP, indicating enhanced solute solubility due to the presence of the co-solvent (10% (w/w) ethanol – water mixture at 57% (v/v)). This is further supported by the higher solubility parameter (y_s) observed in RGP ($1.9202 \cdot 10^{-3}$ kg/kg CO_2) compared to WGP ($1.0357 \cdot 10^{-3}$ kg/kg CO_2), reflecting a greater concentration of extractable compounds in RGP.

The initial mass transfer coefficients (k_fa_0) was slightly lower for WGP ($2.1103 \cdot 10^{-2}\ s^{-1}$) than for RGP ($2.2321 \cdot 10^{-2} \cdot s^{-1}$), suggesting slower external mass transfer for WGP during the CER period. This trend is consistent with the lesser slope of the WGP extraction curve depicted in Fig. 2b.

The solid-phase mass transfer coefficient (k_sa_s) was higher in RGP ($6.3305 \cdot 10^{-6}\ s^{-1}$) than in WGP ($5.6413 \cdot 10^{-6}\ s^{-1}$) confirming what just previously reported for $SC–CO_2$ extraction. The k_fa_0 values are approximately four orders of magnitude greater than the k_sa_s ones for both pomaces, highlighting the dominance of internal diffusion resistance. However, it is interesting to note that the difference between k_fa_0 and k_sa_s values of $SC–CO_2$ + co-solvent extraction compared to $SC–CO_2$ extraction is reduced by about one order of magnitude, suggesting a reduction in internal mass transfer resistance when a co-solvent is used. This effect may be attributed to structural modifications of the pomace induced during the initial $SC–CO_2$ extraction step, in which nonpolar compounds are removed, potentially increasing matrix porosity and facilitating co-solvent penetration. Additionally, co-solvent-induced matrix swelling and enhanced solute–matrix interactions may further contribute to improved internal diffusion. The reduction in internal mass transfer resistance is quantitatively supported by the lower values of the internal resistance parameter Θi, which were calculated as 111.26 for WGP and 101.00 for RGP. Lower Θi values indicate a diminished contribution of internal diffusion limitations to the overall mass transfer process, confirming that the presence of a co-solvent enhances mass transport within the solid matrix.

Notably, WGP exhibited significantly higher values of q_m (44.84 kg CO_2/kg pomace) and q_n (190.80 kg CO_2/kg pomace) compared to RGP (23.47 and 102.44 kg CO_2/kg pomace, respectively). These higher values indicate that WGP required a substantially larger amount of solvent to complete the extraction. This behavior can be attributed to a combination of lower solute accessibility and slower mass transfer

Table 3 Bioactive compounds from white and red grape pomace via SFE sequential process

Sequential SFE process	Bioactive compounds	White grape pomace	Red grape pomace
SC–CO_2 extraction	1-Hexacosanol (mg/kgDM)	1460 ± 97	860 ± 56
	1-Octacosanol (mg/kgDM)	1202 ± 18	749 ± 35
	1-Triacontanol (mg/kgDM)	736 ± 84	232 ± 42
	Total Policosanol (mg/kgDM)	3398 ± 42	1841 ± 15
SC–CO_2 + co-solvent extraction	Total Polyphenols (mgGAE/100gDM)	1879 ± 53	2160 ± 11

kinetics in the WGP matrix. In particular, WGP—typically subjected to less intensive maceration and fermentation—may retain a more intact and hydrophilic cell-wall structure, resulting in stronger binding of polar compounds and higher internal diffusion resistance. Additionally, differences in matrix composition and water retention may reduce the effective mobility and local availability of the ethanol–water co-solvent within the solid phase, thereby decreasing apparent solubility and delaying extraction exhaustion. In contrast, the more disrupted structure of RGP pomace likely enhances solvent penetration and solute desorption, allowing extraction completion at lower solvent-to-solid ratios.

Chemical Composition of Sequential SFE Extracts

The major bioactive compounds extracted from WGP and RGP using the proposed sequential SFE process are shown in Table 3.

In the first step, SC–CO_2 extraction efficiently recovered policosanols, including 1-hexacosanol, 1-octacosanol, and 1-triacontanol. The total policosanol content reached 3398 ± 42 mg/kg DM for WGP and 1841 ± 15 mg/kg DM for RGP, corresponding to approximately 5% and 2.3% of the overall extraction yields, respectively. These results are significant both qualitatively and quantitatively, demonstrating that grape pomace—alongside established sources such as beeswax yellow (5200 mg/kg, with 860, 900, and 2300 mg/kg of the same compounds, respectively) and sugarcane peel (270 mg/kg total policosanol, including 23, 219, and 16 mg/kg of 1-hexacosanol, 1-octacosanol, and 1-triacontanol, respectively) [13]—can be regarded as a valuable source of policosanol.

In the second step of the sequential SFE process, using SC–CO_2 + co-solvent, polyphenols were successfully recovered from grape pomace. The total polyphenol content reached 1879 ± 53 mg GAE/100 g DM for WGP and 2160 ± 11 mg GAE/100 g DM for RGP. For comparison, conventional methanol extraction—reported by Pinelo et al. [38] as the most selective solvent for phenolic compounds—yielded 2087 ± 24 mg GAE/100 g DM for WGP and 2400 ± 43 mg GAE/100 g DM for RGP. Thus, the SC–CO_2 + co-solvent extraction achieved approximately 90% of the polyphenol recovery obtained with methanol, demonstrating its high efficiency.

There is strong market interest in both policosanols and polyphenols, with robust growth forecasts. The global policosanol market is expected to grow at an annual rate of 6–7% through 2030 and beyond, reaching an estimated USD 500–600 million [39]. The global polyphenols market is a significant and growing industry, projected to reach between USD 2.1 billion and USD 3.0 billion by 2030 with a CAGR of approximately 7–8% [40].

Meeting this growing demand requires high-quality, traceable, and sustainably sourced extracts. The sequential SFE process aligns well with these requirements, providing a green, efficient, and advanced technology for the targeted recovery of high-value bioactives from an agro-industrial by-product.

Conclusions

Sequential SFE proved effective for the selective recovery of policosanols and polyphenols from white and red grape pomace. Kinetic modeling with BIC and Sovová's models accurately described the extraction behavior, confirming that internal diffusion resistance governs mass transfer, though co-solvent addition enhanced solubility and reduced diffusion limitations. Red grape pomace showed higher overall yields and phenolic content, while white grape pomace was richer in policosanols, reflecting compositional differences between matrices. The extracts contained bioactives of strong industrial relevance, comparable to conventional commercial sources. Overall, sequential SFE offers a sustainable, efficient, and scalable strategy to valorize grape pomace into high-quality functional ingredients for food, pharmaceutical, and cosmetic applications.

Author Contributions Carla Da Porto: Conceptualization, Writing—Original Draft, Visualization, Supervision, Project administration. Andrea Natolino: Methodology, Formal analysis, Investigation, Writing—Original Draft, Data Curation.

Funding Open access funding provided by Università degli Studi di Udine within the CRUI-CARE Agreement. The authors declare that

no funds, grants, or other support were received during the preparation of this manuscript.

Data Availability Experimental data pertinent to this study can be made available upon reasonable request.

Declarations

Conflict of interest The authors declare no relevant financial or non financial interests.

References

1. International organization of vine and wine (OIV), state of the world vine and wine sector 2024
2. Jin, B., Kelly, J.M.: Wine industry residues. In: Pandey, A.A., Nigam, P.S.N. (eds.) Biotechnology for Agro-Industrial Residues Utilisation: Utilisation of Agro-Residues, pp. 293–311. Springer, The Netherlands (2009)
3. Perra, M., Bacchetta, G., Muntoni, A., De Gioannis, G., Castangi, I., Rajha, H.N., Manca, M.L., Manconi, M.: An outlook on modern and sustainable approaches to the management of grape pomace by integrating green processes, biotechnologies and advanced biomedical approaches. J. Funct. Foods **98**, 105276 (2022). https://doi.org/10.1016/j.jff.2022.105276
4. Beres, C., Costa, G.N., Cabezudo, I., da Silva-James, N.K., Teles, A.S., Cruz, A.P., Freitas, S.P.: Towards integral utilization of grape pomace from winemaking process: a review. Waste Manag. **68**, 581–594 (2017). https://doi.org/10.1016/j.wasman.2017.07.017
5. Da Porto, C., Natolino, A., Scalet, M.: Improved sustainability in wine industry byproducts: a scale-up and economical feasibility study for high-value compounds extraction using modified SC–CO_2. ACS Omega (2022). https://doi.org/10.1021/acsomega.2c02631
6. Ilyas, T., Chowdhary, P., Chaurasia, D., Gnansounou, E., Pandey, A., Chaturvedi, P.: Sustainable green processing of grape pomace for the production of value-added products: an overview. Environ. Technol. Innov. **23**, 101592 (2021). https://doi.org/10.1016/j.eti.2021.101592
7. Jin, Q., O'Keefe, S.F., Stewart, A.C., Neilson, A.P., Kim, Y.T., Huang, H.: Techno-economic analysis of a grape pomace biorefinery: production of seed oil, polyphenols, and biochar. Food Bioprod. Process. **127**, 139–151 (2021). https://doi.org/10.1016/j.fbp.2021.02.002
8. Yaashika, P.R., Senthil Kumar, P., Varjani, S.: Valorization of agro-industrial wastes for biorefinery process and circular bioeconomy: a critical review. Bioresour. Technol. **343**, 126126 (2022). https://doi.org/10.1016/jbiortech.2021.126126
9. Mendes, J.A.S., Prozil, S.O., Evtuguina, D.V., Lopes, L.P.C.: Towards comprehensive utilization of winemaking residues: characterization of grape skins from red grape pomaces of variety Touriga Nacional. Ind. Crop Prod. **43**, 25–32 (2013). https://doi.org/10.1016/j.indcrop.2012.06.047
10. Zhang, M., Zhang, P., Lu, S., Ou-yang, Q., Zhuge, Y., Tian, R., Jia, H., Fang, J.: Comparative analysis of cuticular wax in various grape cultivars during berry development and after storage. Front. Nutr. **8**, 817796 (2021). https://doi.org/10.3389/fnut.2021.817796
11. Yang, M., Luo, Z., Gao, S., Belwal, T., Wang, L., Qi, M., Ban, Z., Wu, B., Wang, F., Li, L.: The chemical composition and potential role of epicuticular and intracuticular wax in four cultivars of table grapes. Postharvest Biol Tech. **173**, 111430 (2021). https://doi.org/10.1016/j.postharvbio.2020.111430
12. Da Porto, C., Natolino, A.: Policosanols from grape marc: a new step towards a sustainable biorefinery for the wine industry by SC–CO_2 extraction. J. CO2 Util. **82**, 102762 (2024)
13. Irmak, S., Dunford, N.T., Milligan, J.: Policosanol contents of beeswax, sugarcane and wheat extracts. Food Chem. **95**, 312–318 (2006). https://doi.org/10.1016/j.foodchem.2005.01.009
14. Dunford, N.T., Edwards, J.: Nutritional bioactive components of wheat straw as affected by genotype and environment. Bioresour. Technol. **101**, 422–425 (2010)
15. Pasha, I., Saeed, F., Waqas, K., Anjum, F.M., Arshad, M.U.: Nutraceutical and functional scenario of wheat straw. Crit. Rev. Food Sci. Nutr. **53**, 287–295 (2013)
16. Wongwaiwech, D., Majai, N., Kamchonemenukool, S., et al.: Comparison of the policosanol contents in commercial health foods and policosanol stability in enriched rice bran oil. Food Prod Process Nutr. **7**, 25 (2025). https://doi.org/10.1186/s43014-024-00303-y
17. Cho, K.H., Bahuguna, A., Lee, S.H., Kim, J.E., Lee, Y., Jeon, C.: Effect of 14-week supplementation of highly purified policosanol (Raydel®) and a sugar cane extract powder (SCEP) on dyslipidemia and oxidative variables in hyperlipidemic zebrafish: insight into liver, kidney, and brain health. Curr. Issues Mol. Biol. **47**, 354 (2025). https://doi.org/10.3390/cimb47050354
18. Olatunji, L.W., Jimoh, A.O., Muhammad, T.U., Imam, M.U.: A review of the effects of policosanol on metabolic syndrome. CCMP **2**, 100058 (2022). https://doi.org/10.1016/j.ccmp.2022.100058
19. Brunner, G.: Supercritical gases as solvents: phase equilibria. Gas extraction: an introduction to fundamentals of supercritical fluids and the application to separation processes, Heidelberg, Steinkopff, 1994
20. Molero Gomez, A., Pereyra Lopez, C., de la Martinez Ossa, E.: Recovery of grape seed oil by liquid and supercritical carbon dioxide extraction: a comparison with conventional solvent extraction. Chem. Eng. J. Bioch. Eng. J. **61**, 227–231 (1996)
21. Brunner, B.: Supercritical fluids: technology and application to food processing. J. Food Eng. **67**, 21–33 (2005)
22. Herrero, M., Cifuentes, A., Ibañez, E.: Sub- and supercritical fluid extraction of functional ingredients from different natural sources: plants. food-by-products, algae and microalgae-a review. Food Chem. **98**, 136–148 (2006)
23. Reverchon, E., De Marco, I.: Supercritical fluid extraction and fractionation of natural matter. J. Supercrit. Fluids **38**, 146–166 (2006)
24. Attard, T.M., McElroy, C.R., Rezende, C.A., Polikarpov, I., Clark, J.H., Hunt, A.J.: Sugarcane waste as a valuable source of lipophilic molecules. Ind. Crops Prod. **76**, 95–103 (2015). https://doi.org/10.1016/j.indcrop.2015.05.077
25. De Melo, M.M.R., Silvestre, A.J.D., Silva, C.M.: Supercritical fluid extraction of vegetable matrices: applications, trends and future perspectives of a convincing green technology. J. Supercrit.

Fluids **92**, 115–176 (2014). https://doi.org/10.1016/j.supflu.2014.04.007
26. Farias-Campomanes, A.M., Rostagno, M.A., Meireles, M.A.A.: Production of polyphenol extracts from grape bagasse using supercritical fluids: yield, extract composition and economic evaluation. J. Supercrit. Fluids **77**, 70–78 (2013)
27. Pereira, C.G., Meireles, A.A.M.: Supercritical fluid extraction of bioactive compounds: fundamentals, applications and economic perspectives. Food Bioprocess Technol. **3**, 340–372 (2010). https://doi.org/10.1007/s11947-009-0263-2
28. Povh, N.P., Marques, M.O.M., Meireles, M.A.A.: Supercritical CO_2 extraction of essential oil and oleoresin from chamomile (*Chamomilla recutita* [L.] Rauschert). J. Supercrit. Fluids **21**, 245 (2001)
29. Sovová, H., Zarevucka, M., Vacek, M., Stransky, K.: Solubility of two vegetable oils in supercritical CO_2. J. Supercrit. Fluids **20**, 15–28 (2001)
30. Sovová, H., Kučera, J., Jež, J.: Rate of the vegetable oil extraction with supercritical CO2-II. extraction of grape oil. Chem. Eng. Sci. **49**, 415–420 (1994)
31. Sovová, H.: Rate of the vegetable oil extraction with supercritical CO_2-I, modelling of extraction curves. Chem. Eng. Sci. **49**, 409–414 (1994)
32. Sovová, H.: Mathematical model for supercritical fluid extraction of natural products and extraction curve evaluation. J. Supercrit. Fluids **33**, 35–52 (2005)
33. Sovová, H.: Broken-and-intact cell model for supercritical fluid extraction: its origin and limits. J. Supercrit. Fluids **129**, 3–8 (2017)
34. Yu, L., Perret, J., Harris, M., Wilson, J., Haley, S.: Antioxidant properties of bran extracts from "Akron" wheat grown at different locations. J. Agric. Food Chem. **51**, 1566–1570 (2003)
35. Haim, D., Berrios, M., Valenzuela, A., Videla, L.A.: Trace quantification of 1-octacosanol and 1-triacontanol and their main metabolites in plasma by liquid-liquid extraction coupled with gas chromatography-mass spectrometry. J. Chromatogr. B **877**, 4154–4158 (2009). https://doi.org/10.1016/j.jchromb.2009.10.034
36. Jin, Q., O'Hair, J., Stewart, A.C., O'Keefe, S.F., Neilson, A.P., Kim, Y.-T., McGuire, M., Lee, A., Wilder, G., Huang, H.: Compositional characterization of different industrial white and red grape pomaces in Virginia and the potential valorization of the major components. Foods **8**, 667 (2019)
37. Deng, Q., Penner, M.H., Zhao, Y.: Chemical composition of dietary fiber and polyphenols of five different varieties of wine grape pomace skins. Food Res. Int. **44**, 2712–2720 (2011)
38. Pinelo, M., Rubilar, M., Jerez, J., et al.: Effect of solvent to-solid ratio on the total phenolic content and antiradical ativity of extracts from different components of grape marc. J. Agric. Food Chem. **53**, 2111–2117 (2005)
39. Future market insights. Policosanol market analysis: size, share, and forecast 2023 to 2033. https://www.futuremarketinsights.com/reports/policosanol-market
40. Polyphenols - global strategic business report., Global industry analysts. https://www.researchandmarkets.com/reports/5030379/polyphenols-global-strategic-business-report

Authors and Affiliations

Carla Da Porto[1] · Andrea Natolino[1]

✉ Carla Da Porto
carla.daporto@uniud.it

[1] Department of Agricultural, Food, Environmental and Animal Sciences, University of Udine, 33100 Udine, Italy